Sensors and Actuators A 234 (2015) 180–187

Contents lists available at ScienceDirect

Sensors and Actuators A: Physical

journal homepage: www.elsevier.com/locate/sna

Stabilization of the tilt motion during capillary self-alignment of rectangular chips

J. Berthier[a,*], K.A. Brakke[b], S. Mermoz[c], C. Frétigny[d], L. Di Cioccio[e]

[a] University Grenoble Alpes F-38000 Grenoble, Department of Biotechnology, CEA, LETI, MINATEC Campus, F-38054, Grenoble, France
[b] Mathematics Department, Susquehanna University, 514 University Avenue, Selinsgrove, PA 17870, USA
[c] STMicroelectronics, 850 rue Jean Monnet, 38926 Crolles Cedex, France
[d] UPMC/CNRS/ESPCI PPMD UMR 7615, Physico-Chimie des Polymeres et des Milieux Disperses, 10 rue Vauquelin, 75231 Paris, Cedex 05, France
[e] University Grenoble Alpes F-38000 Grenoble, Department of Microelectronics, CEA, LETI, MINATEC Campus, F-38054, Grenoble, France

ARTICLE INFO

Article history:
Received 24 February 2015
Received in revised form 4 September 2015
Accepted 4 September 2015
Available online 7 September 2015

Keywords:
Capillary self-alignment (CSA)
Alignment modes
Tilt mode
Stabilization
Lyophilic bands

ABSTRACT

Capillary self-alignment (CSA) has emerged as a convenient technique to assemble solid objects. In this technique a liquid droplet forces a mobile solid plate or chip to align with its counterpart on a solid substrate. It has been widely investigated for applications such as 3D microelectronics and assembly of optical components. It is now thought that it could be a solution for surface mounting and packaging technologies. For 3D microelectronics, where square or rectangular chips are used, it has been found that amongst the four displacement modes, i.e. shift, twist, lift and tilt, only the tilt mode was unstable (not restoring). In particular, tilting of a floating square or rectangular chip may trigger a direct contact between the plate and the pad that impedes alignment. In this text, an analysis of the tilt mode is first presented. Second, it is demonstrated that tilt can be stabilized by incorporating specific geometrical features such as lyophilic bands patterned on the substrate.

1. Introduction

Capillary self-alignment (CSA) of mesoscopic objects emerged in the early 1990s as a convenient technique to assemble solid objects [1–4]. It has been recently widely investigated for applications such as 3D microelectronics [5–7] and assembly of optical components [8–10]. It is now thought that it could be a solution for packaging technologies [11]. In this technique the capillary forces exerted by a liquid sandwiched between the two plates forces the mobile solid plate or chip to align with its counterpart on the solid substrate. More specifically, surface tension forces associated to capillary pinning create restoring forces and torques that tend to bring the moving part into alignment [12–14]. Later, evaporation—when the liquid is water—or solidification—when the liquid is a solder—immobilizes the chip in the aligned position.

In the particular case of 3D microelectronics, where square or rectangular chips are used (Fig. 1), it has been found that amongst the four displacement modes—shift, twist, lift and tilt—the three first were stable (restoring). On the other hand, the effect of the tilt mode has been lengthily debated. Using sophisticated calculation, it appeared that this mode is slightly unstable (not restoring) [13]. Fig. 2 shows the tilting of a LED deposited on a solder. The instability of the tilt mode may bring serious drawbacks on the capillary alignment technique [13–19]. For 3D microelectronics, where small amounts of liquid are used, the distance between the two solids is small, and tilting may trigger a direct contact between the moving plate and the fixed pad that impedes alignment. Avoiding tilt requires achieving perfect horizontality of the chip at the instant of the drop-off, which complicates substantially the robotics that brings the chip above the pad [20].

Self-alignment of mirrors uses the same capillary principle as microelectronic chip alignment [7–9]. In the alignment process of mirrors for optical applications, a solder is used, then gelled, and tilt cannot be tolerated. Fig. 2 shows an example of tilt instability during the alignment of mirrors.

Other approaches for the control of the tilt have been done: mechanical stops and hinges for the guidance of the pieces to assemble have been shown to be effective against rotational undesired motion [21,22]. However, due to their 3D structure, such devices require complicated fabrication, not compatible with the requirements of microelectronics. Note that for very small objects to align—in the range from 50 to 200 μm where random agitation is efficient—hydrophobic patterns on the objects have been used to improve the alignment [23]. This type of solution is not effective

* Corresponding author.
E-mail address: jean.berthier@wanadoo.fr (J. Berthier).

http://dx.doi.org/10.1016/j.sna.2015.09.008
0924-4247/

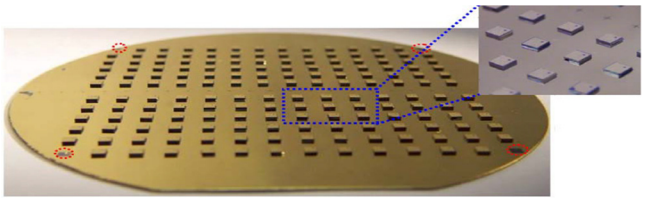

Fig. 1. Chips self-assembled on a wafer.

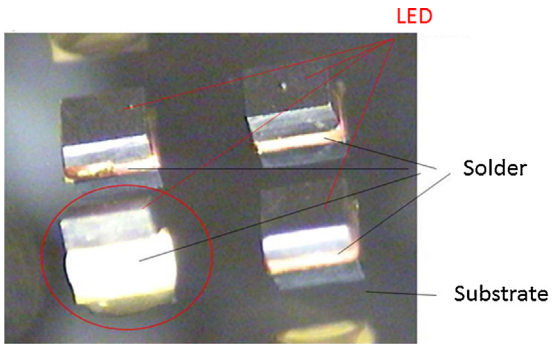

Fig. 2. Left: tilting of a LED deposited on a liquid solder.

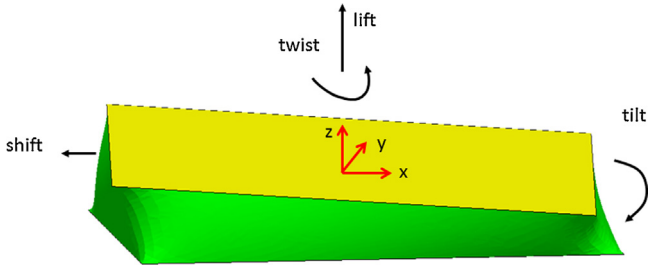

Fig. 3. The four displacement modes during alignment process.

for microelectronic chips whose size is much larger—in the range 1–5 mm—and for which random agitation is not conceivable.

Based on a computational approach, a completely passive method is described in this work that impedes the tilt motion for square and rectangular chips.

First an analysis of the tilt mode is presented: it shows that the tilt mode is slightly unstable in the case of square or rectangular chips [13]. Second, it is demonstrated that tilt can be eliminated by incorporating specific geometrical features such as wetting bands patterned on the substrate. These wetting bands allow for a controlled spreading of the liquid.

The solution is completely passive and does not bring complication in the microfabrication process. It just requires drawing a patterning mask that includes the wetting bands.

2. Alignment modes

In the process of alignment of square or rectangular chips, four displacement modes have been defined: (1) shift, which is a horizontal translation of the plate, (2) twist, corresponding to a rotation of the plate in the horizontal plane, (3) lift, corresponding to a vertical motion of the plate, and (4) tilt and roll, which are respectively rotations around the horizontal y-axis and x-axis (Fig. 3).

An analysis of the restoring forces and torques has been done analytically [13,20] and in addition numerically by using the program Surface Evolver [24]. Fig. 4 shows the restoring of alignment for shift, lift and twist modes, but not for the tilt mode. In the following, we investigate the physics of the tilt mode and propose a geometrical solution to render the tilt mode stable for chips of sufficiently light weight.

3. Analysis of the tilt mode

By definition, tilt is a rotation around the y-axis and roll a rotation around the x-axis. Basically, tilt and roll share the same behavior. In the case where the chip has a square shape, tilt and roll are exactly identical. Tilt is a complex phenomenon because the variation of the surface area is difficult to intuitively predict.

If we make the very simple reasoning presented in Fig. 5, comparing horizontal and fully tilted chip positions, we deduce that the problem is indeterminate. For the same volume of liquid, we assume the simplest form of surfaces: flat interfaces in the case of parallel-to-pad chip, and in the case of the dihedral position, a cylindrical interface for the largest surface area, and flat interfaces for the two lateral surfaces. The surface energy E in the horizontal configuration is

$$E = \gamma S = \gamma\,(4\,L\,h) = \gamma\left(4\,\frac{V_l}{L}\right), \tag{1}$$

where V_l is the liquid volume, L the dimension of the pad—and chip—edge, and γ the liquid–air surface tension. In the dihedral morphology, the surface energy is

$$E = \gamma S = \gamma\left[2\left(\frac{\alpha L^2}{2}\right) + \alpha L^2\right] = \gamma\left(4\,\frac{V_l}{L}\right), \tag{2}$$

where α denotes the dihedral angle.

The two calculated energies are equal. Hence, it is the distortion of the surfaces that can make the difference and pinpoint the stable position. It is a second order problem that requires a careful numerical approach. This remark leads to serious complications: from a numerical standpoint, the meshing of the surface should be sufficiently fine and the numerical method should be sufficiently elaborated to produce a precise value of the energy. In return, the computation time is long. From a physical standpoint, the roles of the parameters—like the weight of the chip, or the surface tension of the liquid—are difficult to predict.

In the investigations presented in this work, we have considered a square chip of horizontal dimensions 5×5 mm, with a weight of 0.07 g (corresponding to a chip height of approximately 400 μm). The liquid is water, with a surface tension $\gamma = 72$ mN/m.

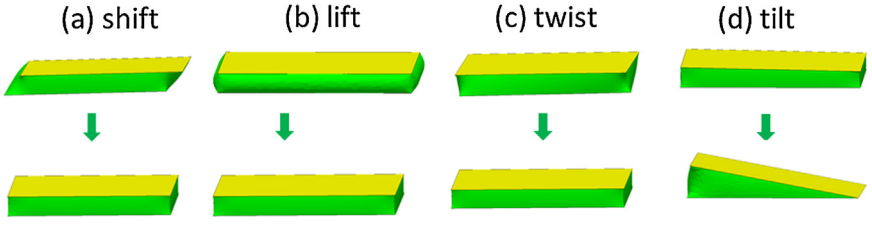

Fig. 4. (a)–(c): Shift, lift and twist modes are stable; tilt mode (d) is unstable (from Evolver).

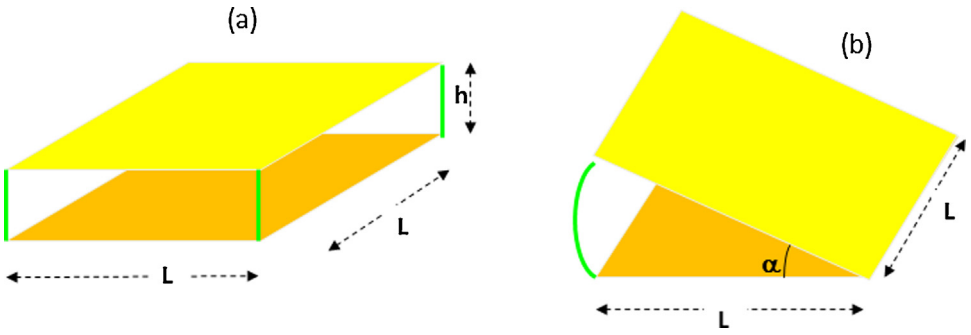

Fig. 5. Two morphologies of the liquid having the same surface energy.

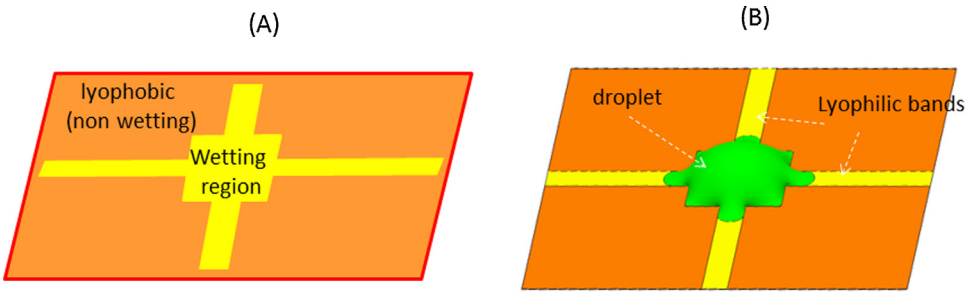

Fig. 6. (A) Sketch of the fixed pad with two wetting bands; (B) Evolver calculation of the shape of a droplet pipetted on the central region.

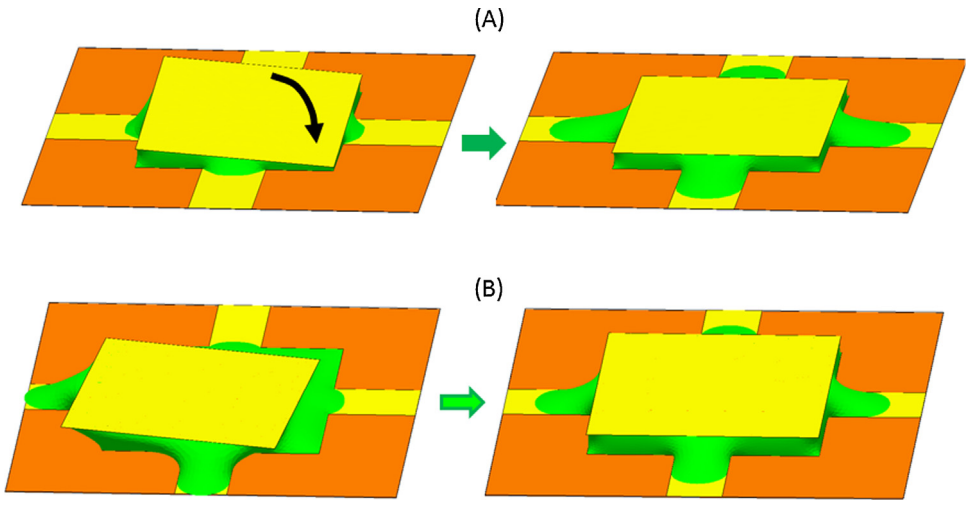

Fig. 7. (A): A square chip realigns horizontally after an initial tilt; (B) the square chip realigns perfectly after an initial combination of shift, twist and tilt motion. Chip dimensions 5 × 5 mm, chip weight 0.07 g.

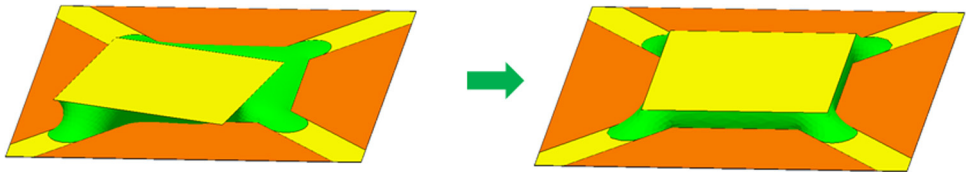

Fig. 8. (A): An initial displacement of a square chip placed above a square pad with diagonal wetting bands is restored by the action of capillary forces and torques.

The numerical model (Evolver) shows that, in absence of stabilizing wetting bands, the dihedral position (denoted (b) in Fig. 5) is the stable position; in other words, the tilt mode is unstable. It is unstable even in combination with other modes, such as shift and twist modes [13].

Fig. 2 is an example of tilt instability during the alignment of chips for optical applications. An energy calculation with the tilt angle is presented in Fig. 9, showing the decrease of surface energy with the tilt angle when no wetting bands are present.

4. Blocking the tilt motion using wetting bands

As one of the main interests of CSA concerns the square chips used in 3D microelectronics—and this shape being tilt-

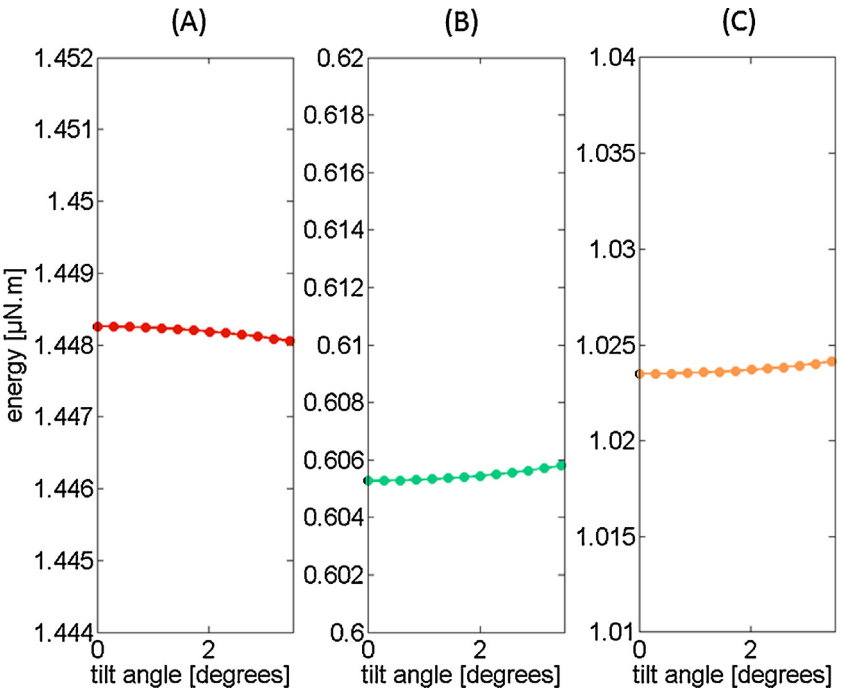

Fig. 9. Interfacial energy vs. tilt angle; (A) square pad with no bands, (B) square pad with perpendicular-to-pad bands, and (C) diagonal bands. The chip weight considered for the calculation is 0.07 g.

unstable—we introduce lyophilic (wetting) bands on the substrate perpendicular to the fixed pad, as shown in Fig. 6A. A droplet deposited on the central region takes the shape shown in Fig. 6B. Liquid fingers spread on the wetting bands, and does not overflow out of the bands if the wettability contrast is sufficient. For the calculation, the contact angle on the patterned bands is set to 20°, the contact angle on the lyophobic substrate 120°, the width of the bands is 1 mm and the wetting region is a square of 5 × 5 mm.

The next step of the numerical approach is the taken into account of the mobile chip. When the chip is placed on top of the liquid, liquid fingers extend on the wetting bands. It is observed that these fingers counteract the tilt motion. Moreover, it is shown that the presence of these bands—if they are not too wide—does not change the restoring properties of the other modes (shift, twist, lift) as shown in Fig. 7.

Note that the disposition of the wetting bands perpendicular to the fixed pad—as in Figs. 6 and 7—can be placed otherwise, for example diagonally, as shown in Fig. 8. We will investigate later the effect of the position of the bands.

The stable position corresponding to a minimum of the energy, the chip is brought back into a horizontal position if the energy decreases with a decreasing tilt angle. Equivalently, the chip is brought back into a horizontal position if the value of the torque defined by

$$T = -\frac{\partial E}{\partial \alpha} = -\gamma \frac{\partial S}{\partial \alpha}, \tag{3}$$

where E is the interfacial energy and α the tilt angle, is negative. It is seen in Fig. 10 that the torque is negative in the case where lyophilic bands are present, the two configurations—diagonals or perpendicular-to-pad bands—producing similar results. On the other hand, the torque is slightly positive when no bands are present. We have considered small initial tilts (less than 4°), but the results can be extrapolate further due to the linearity of the curves; note that the maximum possible tilt when the chip touches the pad is 10°.

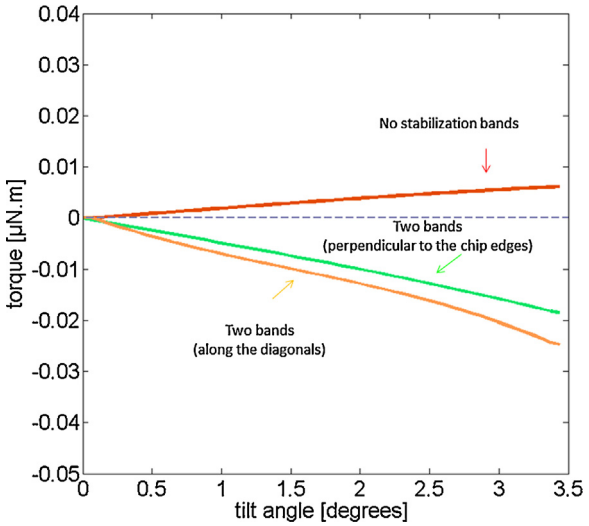

Fig. 10. Tilt torques vs. tilt angle; red curve corresponds to square pad with no bands, green curve to square pad with perpendicular-to-pad bands, and yellow curve to diagonal bands. The two last cases show a negative, i.e. restoring torque. (For interpretation of the references to colour in this figure legend, the reader is referred to the web version of this article.)

The physical reason behind the restoring torque caused by the bands is not straightforward. We present here a tentative physical explanation. Let us start with a pad with only one lyophilic band, as shown in Fig. 11. The capillary forces on the triple line on the band trigger the extension of liquid fingers. Any random perturbations of the initially horizontal position of the chip—for example a tilt and a roll—results in the tipping of the chip due to an increase of the tilt; the roll is however cancelled by the presence of the lyophilic band.

Let us consider now a tilt of the chip in the case of two perpendicular-to-pad bands. The Laplace pressure is determined by the curvature radii in the horizontal (R_h) and vertical plane (R_v). Whereas the vertical curvatures are similar, the horizontal curva-

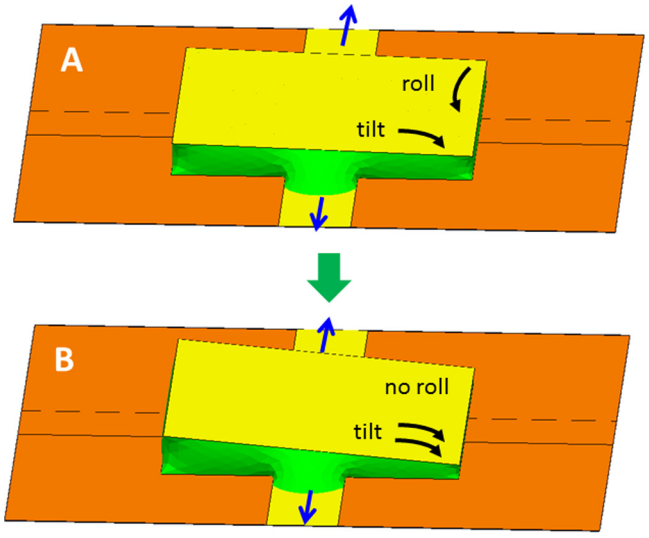

Fig. 11. In the case where only one lyophilic band is present, any perturbation in the initially horizontal position (A) is increased in the direction perpendicular to the band (tilt), and decreased in the direction of the band (roll) as shown in (B). The blue arrows symbolize the capillary forces on the triple line located on the band.

ture is much higher for a deeper finger (Fig. 12). So the tilted up side has the higher curvature and the higher pressure. Hence the fluid is driven out into the shallower fingers, decreasing the tilt until horizontal stabilization. A very intuitive way to explain the stabilization is to imagine that the bands act as "ropes" exerting lateral forces of the moving chip.

5. Effect of the bands on the other modes

In order to be effective, the presence of wetting bands should keep all the other displacement modes—shift and twist—restoring. In this section, we show that the introduction of the wetting bands does not change substantially the restoring capacities of the other modes. In Fig. 13 we compare the effect of the bands on the shift and twist modes.

In all cases the shift and the twist modes are restoring, because the capillary forces and torques are negative. Note that the two configurations—diagonal or perpendicular-to-pad bands—are equivalent for the shift force and the twist restoring torque is somewhat larger for the diagonal bands.

6. Influence of the chip weight on the tilt

With the application to 3D microelectronics in mind, we have considered so far a chip weight of 0.07 g, corresponding approximately to a silicon chip of 5×5 mm $\times$ 500 μm. Other applications, such as the optical applications sometimes require heavier mobile plates (Fig. 2).

It has been observed—in the reference case of a pad without any wetting bands—that the tilt instability was increased by a larger chip weight [13]. Then the question is: would the wetting bands still stabilize the tilt motion in the case of large chip weight?

In order to answer this question, we have investigated the stability to tilt for two different chip weights: 0.07 and 0.1 g. The results are plotted in Fig. 14. It is observed that an increase of the chip weight decreases the value of the restoring torque—when the torque is restoring, and increases the tilt instability—when the torque is not restoring. In our case, for a 5×5 mm chip, the weight of the chip should not be larger than approximately 0.13 g to benefit from a tilt-restoring torque.

7. Influence of the width of the bands

Another question can be raised: what is the best bandwidth to ensure tilt-stability? It is clear that if the ratio between the bandwidth w and the length of the square pad edge L decreases to zero, the effect of the bands disappears. Fig. 15 shows the restoring torques for widths $w = \{0.58\,\text{mm}, 0.71\,\text{mm}, 1.3\,\text{mm}, 1.8\,\text{mm}\}$, corresponding to the ratios $w/L = \{0.12, 0.14, 0.25, 0.36\}$. The larger the widths of bands, the higher the value of the restoring torque, until approximately a value of the ratio $w/L \sim 0.35$. Interestingly, the ratio $w/L \sim 0.35$ does not deteriorate the restoring effect of the two other modes (shift and twist), as shown in Fig. 16.

8. Influence of the contact angle

Finally we analyze the effect of the contact angle on the magnitude of the restoring torques. Using continuity arguments, contact angles close to 90° are equivalent to a situation without wetting

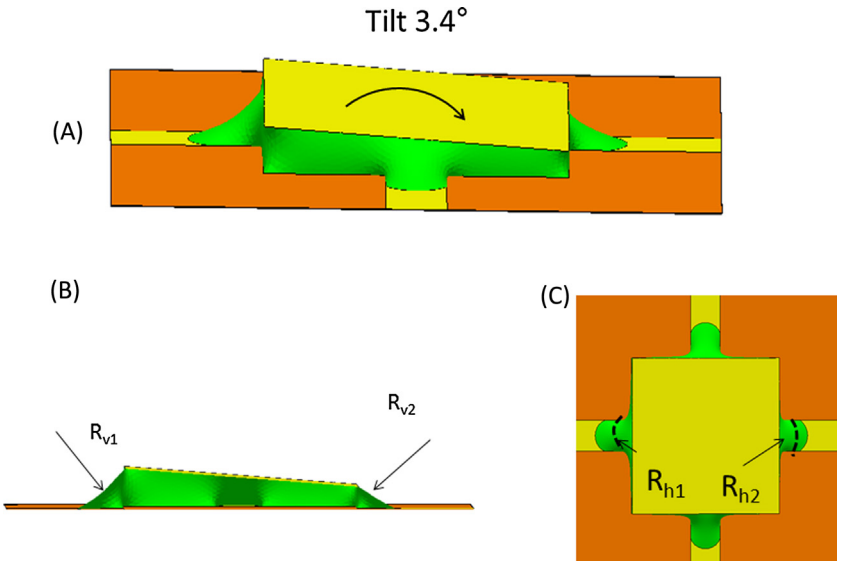

Fig. 12. (A): View of the tilted chip; (B), sketch of the two vertical curvatures which are very similar; note that the angle of the surface is much more vertical at the top on the left, providing a restoring torque; (C) view of the horizontal curvature radii, showing the inequality $R_{h1} < R_{h2}$.

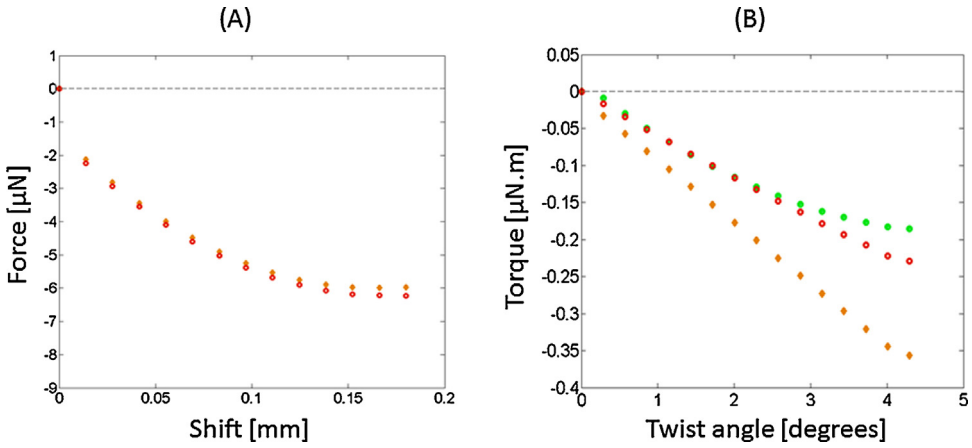

Fig. 13. Shift and twist are restoring in all cases. (A) shift mode and (B) twist mode; Evolver comparison between square pad (red dots), perpendicular-to-pad bands (green dots) and diagonal bands (orange dots). (For interpretation of the references to colour in this figure legend, the reader is referred to the web version of this article.)

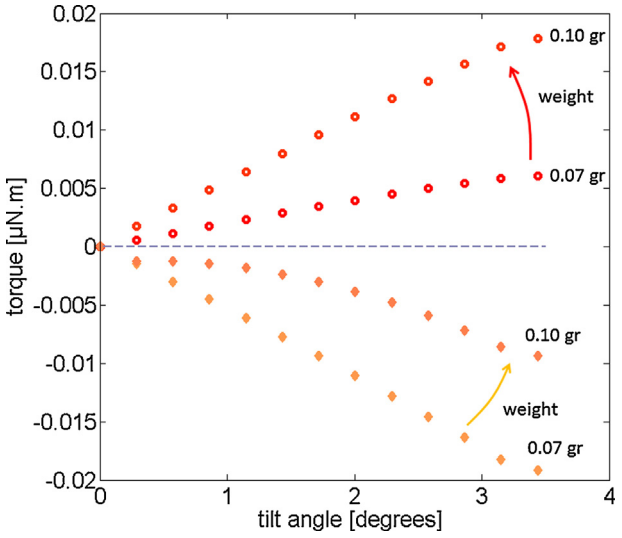

Fig. 14. An increase in the weight of the mobile chip decreases the stability of the tilt mode (the two top curves correspond to the no-band case, and the two bottom curves to diagonal bands, contact angle 20°, width of bands 0.07 mm).

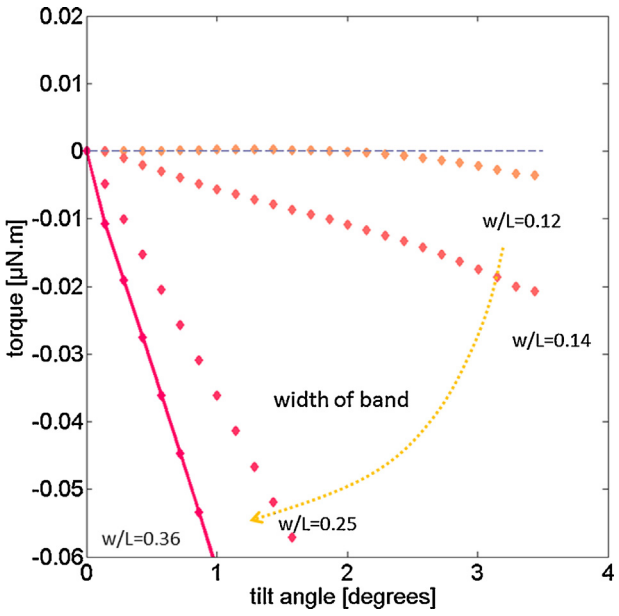

Fig. 15. The restoring torque increases with the width of the bands (case of diagonal bands, contact angle 20°, chip weight 0.07 g, chip dimensions 5 × 5 mm).

bands. Small contact angles are needed to obtain a restoring torque, as was proved by the Laplace analysis conducted above.

Fig. 17 shows an increase of the magnitude of the restoring torque with a decreasing contact angle, confirms this analysis. Remark that small contact angles are the rule for CSA, because liquid spreading on the chip and pad must be efficient [17], besides in the case of 3D microelectronics, hydrophilic surfaces facilitate the direct bonding of the two solids.

9. Discussion and conclusion

In the technique of capillary self-alignment (CSA) for 3D microelectronics where square or rectangular chips must be aligned above geometrically corresponding pads, it is known that the tilt mode is slightly unstable. Hence an initial tilt—occurring at the moment of chip release on the liquid—cannot be restored and the achievement of alignment can be impossible due to a mechanical contact of the chip with the pad.

It is shown in this text that the use of two lyophilic bands patterned on the pad changes the unstable tilt mode into a restoring mode, at the condition that the chip weight is not too large. Heavy chips would always be subject to tilt instability. Moreover, optimal values of the system parameters, such as the width of the bands and the value of the contact angle have been determined. Different geometries for the bands are possible. We have studied the two most straightforward geometries, i.e. perpendicularly-to-pad and diagonal bands. If the chip weight is not too large, the use of such additional bands renders all displacement modes stable—i.e. any departure from alignment is automatically restored.

From a microfabrication standpoint, the lyophilic bands do not bring complications in the micro-fabrication process; they just require a patterning mask that takes into account these bands. Two different patterning of the fixed substrate can be readily envisioned: hydrophilic pads connected or not by perpendicular stripes, as shown in Fig. 18. Additional studies must be conducted to investigate which of the two designs is the most effective.

For any of the two geometries depicted in Fig. 18, the microfabrication process is similar, and is described in Fig. 19.

Acknowledgements

This work has been done in the frame of cooperation between CEA (Grenoble, France), University Pierre and Marie Curie (Paris,

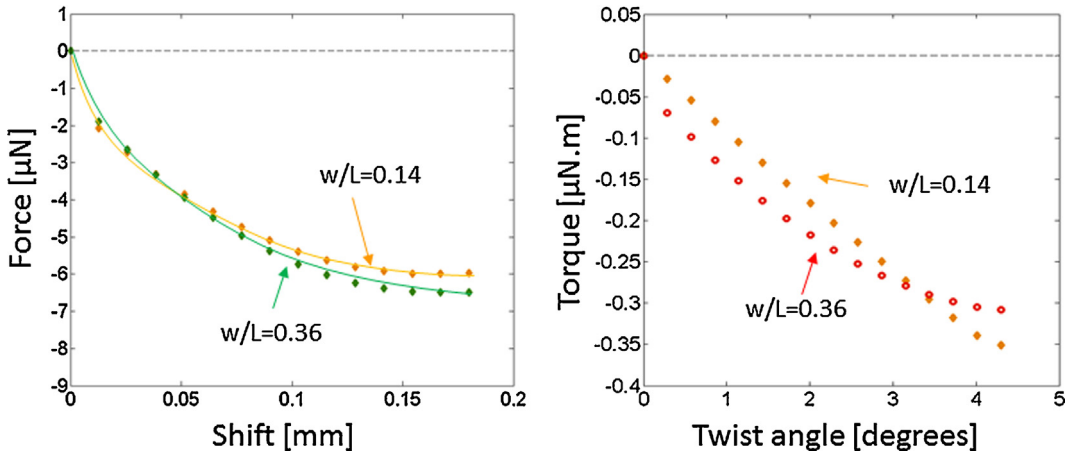

Fig. 16. Left: shift restoring force for two different widths of band (w/L = 0.14 and 0.36); right: twist restoring torque for the two same bands.

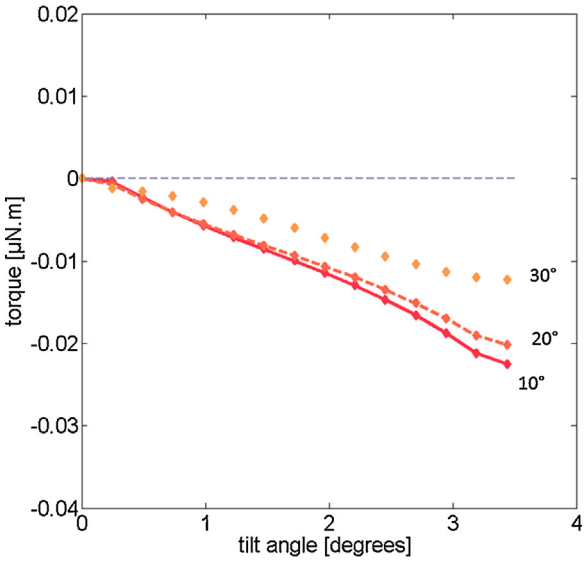

Fig. 17. Tilt-restoring torque vs. liquid contact angle with the bands (case of diagonal bands, width of bands 0.7 mm, chip weight 0.07 g).

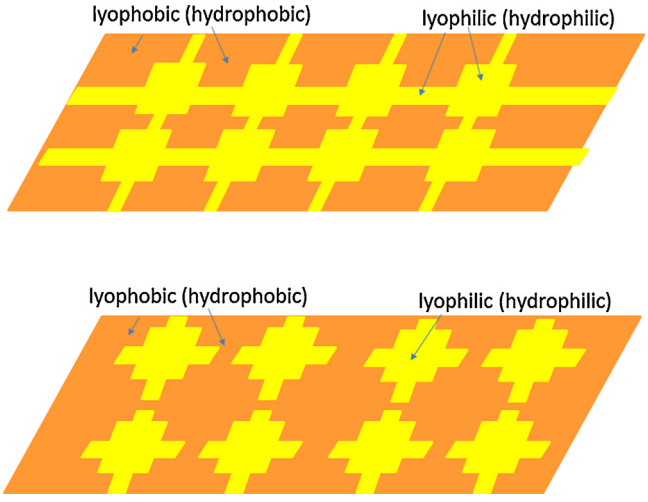

Fig. 18. Two different possible geometries for the patterning of the fixed substrate.

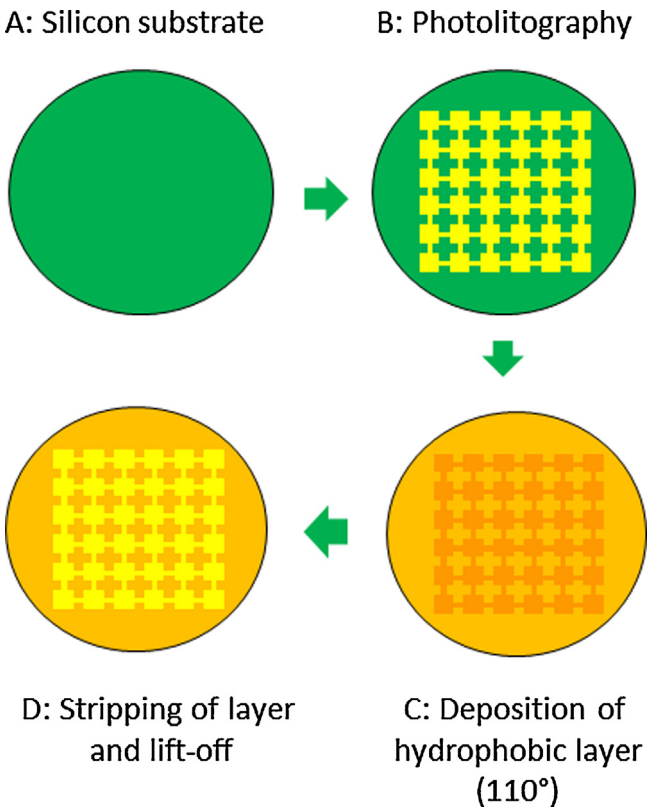

Fig. 19. Schematic of the microfabrication.

France), ESPCI (Paris, France) and STMicroelectronics (Grenoble, France). We thank Ken Brakke (Susquehanna University) for his collaboration in this project.

References

[1] G.M. Whitesides, M. Boncheva, Beyond molecules, PNAS 99 (2002) 4769.
[2] G.M. Whitesides, B. Grzybowski, Self assembly at all scales, Science 295 (5564) (2002) 2418–2421.
[3] M.J. Wale, C. Edge, F.A. Randle, D.J. Pedder, A new self-aligned technique for the assembly of integrated optical devices with optical fibre and electrical interfaces, in: 15th European Conf. Optical Communications, Gothenburg, Sweden, 10–14 September 1989, 2015, pp. 368–371.
[4] M.J. Wale, C. Edge, Self-aligned flip-chip assembly of protonic devices with electrical and optical connections, IEEE Trans. Compon. Hybrids Manuf. Technol. 13 (4) (1990) 780–786.

[5] J.A. Pelesko, Self-assembly: The Science of Things That Put Themselves Together, Chapmann & Hall/CRC, 2007.
[6] Q.Y. Tong, Q.U. Gösele, Semiconductor Wafer Bonding, Wiley, 1999.
[7] T. Fukushima, E. Iwata, T. Konno, J.-C. Bea, K.-W. Lee, T. Tanaka, M. Koyanagi, Surface tension-driven chip self-assembly with load-free hydrogen fluoride-assisted direct bonding at room temperature for three-dimensional integrated circuits, Appl. Phys. Lett. 96 (2010) 154105.
[8] A. Avital, Zussman, Fluidic assembly of optical components, IEEE Trans. Adv. Packag. 29 (4) (2006) 719.
[9] S.N. Reznik, W. Salalha, A.L. Yarin, E. Zussman, Microscale fiber alignment by a three-dimensional sessile drop on a wettable pad, J. Fluid Mech. 574 (2007) 179–207.
[10] A. Takei, Y. Yoshihata, I. Shimoyama, Microprism using capillary alignment, J. Micromech. Microeng. 21 (2011) 085009.
[11] T. Fukushima, T. Konno, E. Iwata, R. Kobayashi, T. Kojima, M. Murugesan, J.-C. Bea, K.-W. Lee, T. Tanaka, M. Koyanagi, Self-assembly of chip-size components with cavity structures: high-precision alignment and direct bonding without thermal compression for hetero integration, Micromachines 2 (49) (2011).
[12] K.F. Böhringer, U. Srinivasan, R.T. Howe, Modeling of capillary forces and binding sites for fluidic self-assembly, in: 14th International Conference Micro Electro Mechanical Systems, Interlaken, Switzerland January 21–25, 2001.
[13] J. Berthier, K. Brakke, F. Grossi, L. Sanchez, L. Di Cioccio, Self-alignment of silicon chips on wafers: a capillary approach, J. Appl. Phys. 108 (2010) 054905.
[14] P. Lambert, M. Mastrangeli, J.-B. Valsamis, G. Degrez, Spectral analysis and experimental study of lateral capillary dynamics for flip-chip applications, Microfluid Nanofluid 9 (2010) 797–807.
[15] G. Arutinov, E.C.P. Smits, M. Mastrangeli, G. van Heck, J. van den Brand, H.F.M. School, A. Dietzel, Capillary self-alignment of mesoscopic foil components for sensor-systems-in-foil, J. Micromec. Microeng. 22 (2012) 115022.
[16] M. Mastrangeli, S. Abbasi, C. Varel, C. Van Hoof, J.-P. Celis, K.F. Böhringer, Self-assembly from milli- to nanoscales: methods and applications, J. Micromech. Microeng. 19 (2009) 083001.
[17] J. Berthier, K. Brakke, S. Mermoz, L. Sanchez, C. Frétigny, L. Di Cioccio, Self-alignment of silicon chips on wafers: a numerical investigation of the effect of spreading and wetting, Sens. Transducers J. 13 (2011) 44–52.
[18] G. Arutinov, E.C.P. Smits, P. Albert, P. Lambert, M. Mastrangeli, In-plane mode dynamics of capillary self-alignment, Langmuir 30 (2014) 13092–13102.
[19] S. Mermoz, L. Sanchez, L. Di Cioccio, J. Berthier, E. Deloffre, C. Fretigny, Impact of containment and deposition method on sub-micron chip-to-wafer self-assembly yield, in: IEEE International 3D System Integration Conference (3DIC), January 31–February 2, Osaka, Japan, 2012.
[20] J. Lienemann, A. Greiner, J.G. Korvink, Surface tension defects in microfluidic self-alignment, Proceedings of the SPIE conference, Design, test, Integration and Packaging of MEMS/MOEMS vol. 4755 (2002).
[21] R.R.A. Syms, C. Gormley, S. Blackstone, Improving yield, accuracy and complexity in surface tension self-assembled MOEMS, Sens. Actuators A (2000) 1–11.
[22] D.J. Filipiak, A. Azam, T.G. Leong, D.H. Gracias, Hierarchical self-assembly of complex polyhedral microcontainers, J. Micromech. Microeng. 19 (7) (2009), 075012.
[23] J.S. Randhawa, L.N. Kanu, G. Singh, D.H. Gracias, Importance of surface patterns for defect mitigation in three-dimensional self-assembly, Langmuir 26 (15) (2010) 12534–12539.
[24] K. Brakke, The surface evolver, Exp. Math 1 (1992).

Biographies

Jean Berthier is a senior scientist at the CEA-LETI-Minatec. He received a MS in mathematics from the University of Grenoble, an engineering diploma from the Institut National Polytechnique in Grenoble and a PhD from the University Pierre et Marie Curie in Paris. After spending four years at Sandia and Los Alamos National laboratories focused on the interaction between liquid and gases, he joined the CEA-Leti in Grenoble, France. He is presently involved in the development of microfluidic solutions for liquid–liquid extraction, bio-encapsulation of living cells and point-of-care devices. He is the first author of the book "Microfluidics for Biotechnology" published by Artech House (edition 2010), the author of the book "Microdrops and Digital Microfluidics" published by William Andrew-Elsevier (second edition 2012), and the first author of the book "The physics of micro-droplets" published by Scrivener-Wiley Publishing in 2012. He is the author of many journal and conferences articles and patents.

Kenneth Brakke earned his Ph.D. in mathematics at Princeton under Fred Almgren, in the field of Geometric Measure Theory, which may be described as the mathematics of ideal soap films and soap bubbles. After a stint at Purdue University, he moved to Susquehanna University, where he is now Degenstein Professor of Mathematical Sciences. His research interest remains soap films and bubbles, centered on his software Surface Evolver, which is a program for modelling soap films and bubbles by minimizing surface energy subject to constraints.

Sébastien Mermoz received a MS degree in engineering physics from the University Joseph-Fourier, Grenoble, France and in 2015, a Ph. D. degree in Material and Semiconductor Physics from the University of Grenoble-Alpes, France. He has recently joined the company STMicroelectronics in Grenoble where he continues his work on 3D microelectronics.

Christian Frétigny is a CNRS researcher at the Ecole Supérieure de Physique et de Chimie (ESPCI) at Paris. He earned is PhD in solid state physics then he moved to the field of soft matter physics. His main research interests concern surface and interface properties of such systems. He developed several projects on adhesion and friction at a submicrometer scale. He has co-authored of a book on local probes microscopies (Les nouvelles microscopies: A la découverte du nanomonde, Belin, Paris). More recently, he is involved in various questions on the effect of confinement on polymer ultra-thin films, the relationship between friction and roughness and the boundary conditions of liquids at solid surfaces.

Lea Di Cioccio received a degree in engineering physics from the Institut National des Sciences Appliquées, Rennes, France, an M.S. degree in metallurgy and material science from Paris VI University in 1985, and a Ph. D. degree in Material and Semiconductor Physics from the Institut National In 1990 she joined the CEA-LETI (Commissariat à l'Energie Atomique et aux Energies Alternatives in the Laboratoire d'Electronique et de Technologies de l'Instrumentation) in Grenoble, where she was first engaged in physical-chemical characterization such as Transmission Electron Microscopy. She is a specialist in semiconductor heterostructures and 3D integration using various processes such as epitaxy, wafer bonding and thinning. She is currently leading, several projects related to aligned and bonded thinned wafers and dice. Her projects have been funded by French public research agencies, the European Commission and by industrial partners. She is author and co-author of more than 150 publications and 30 patents. She has written several book chapters e.g. on wafer bonded heterostructures in "Wafer Bonding Applications and Tchnology" and a 3D review chapter in Handbook of 3D Integration, Technology and Applications of 3D Integrated Circuits, published by Wiley.